The International Journal of Advanced Manufacturing Technology (2018) 96:4445–4453
https://doi.org/10.1007/s00170-018-1921-1

ORIGINAL ARTICLE

Research on transition region in sectional multi-point forming of saddle-shaped parts

Mingyang Cui [1,2] · Mingzhe Li [1,2] · Erhu Qu [1,2] · Chengxiang Zheng [1,2] · Yunming Sun [1,2]

Received: 5 November 2017 / Accepted: 15 March 2018 / Published online: 26 March 2018

Abstract
The design of the transition region is significant for effective sectional multi-point forming (SMPF) of sheet metal. In this work, the characteristics of the SMPF and design of the transition region in SMPF were systematically studied, and the reasonable design scheme of transition region is summarized. Numerical simulations of a saddle-shaped workpiece formed with different transition region design schemes were performed with finite element analysis software and compared with the design without the transition region. The results show that the reasonable design of the transition region can effectively inhibit indentation and wrinkle defects in the sheet metal during the SMPF process. The values of stress and strain were found to be smaller with uniform distribution compared to the design without the transition region. The flow of sheet metal was also more uniform and the distribution of thickness more reasonable. Finally, a series of experiments on 2024 aluminum alloy sheet metal were tested on the multi-point forming press (MPF) to verify the accuracy of simulation results. The results conclusively prove that the reasonable transition region design can greatly improve the forming effect of sectional forming.

Keywords Multi-point forming · Sectional forming · Transition region · Numerical simulation · Indentation

1 Introduction

The sectional multi-point forming (SMPF) process makes full use of the discrete and deformable forming features of MPF equipment [1, 2]. In the case that a large workpiece is not separated, it is formed section-by-section on the small equipment. However, the indentation, wrinkling, and springback are the main defects when forming large-size sheet metal in SMPF [3–5]. To process a good quality workpiece, designing the transition region of the forming dies is necessary. The transition region acts as a buffer in the forming process, and the forming defects can be effectively reduced.

A group of international and domestic academics has intensely researched the forming of large-size sheet metal [6, 7]. Traditional method uses a line heating technique to form large sheet metal. In one study, Moshaiov [8] investigated the process and developed theoretical support for the production of large-size sheet metal. Dong Dashuan et al. [9] performed intensive research on the line heating technique using the finite element numerical simulation analysis method. Although the line heating technique is mature for the production of large sheet metal, this method is time- and energy-consuming and has higher technical requirements for the operator. In order to solve these problems, Li Mingzhe et al. [1, 10] proposed the method of forming large-size sheet metal using multi-point forming equipment, where the multi-point dies are adjusted according to the shape of the workpiece. The large-size sheet metal is then formed by SMPF, which greatly improves the production efficiency and quality of the forming parts [11–13]. In addition, Chen Jianjun et al. [14] obtained preliminary theoretical findings on the key design of the transition region in SMPF.

Recent developments and research on MPF technology of sheet metal have shown that the forming quality of large-size sheet metal is getting increasingly better [15, 16]. In this paper, the optimum design of transition region in SMPF is presented. Numerical simulations of a saddle-shaped workpiece designed with a transition region were performed with finite element analysis software, and the forming results were

✉ Mingzhe Li
limz@jlu.edu.cn

[1] Dieless Forming Technology Center, Roll Forging Institute, Jilin University, Changchun 130025, China

[2] College of Materials Science and Engineering, Jilin University, Changchun 130025, China

Fig. 1 The work surface of YAM-200 multi-point forming press

compared with those obtained without the design of the transition region. The conclusive feasibility and versatility of the design scheme of the transition region were proven experimentally.

2 The method of SMPF

MPF is a novel forming process for curved surface parts, which is proposed based on the flexible method. Based on the digital information of a workpiece, the shape of the corresponding multi-point dies can be adjusted. The use of SMPF in multi-point dies can realize rapid, continuous, and digital forming of large 3D curved surface parts. As shown in Fig. 1, the YAM-200 MPF press, developed by Jilin University, allows the required shape of dies to be fine-tuned by adjusting equipment, and the sheet metal is formed by loading the upper die.

When performing SMPF, the sheet forming can be divided into four regions, including effective deformed, transition, free deformed, and rigid regions. Figure 2 shows the relationship among the four forming regions after the first sectional

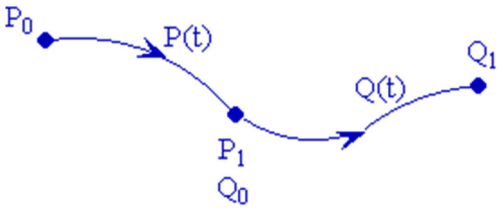

Fig. 3 Two function curves $P(t)$ and $Q(t)$

forming of a large-size saddle-shaped workpiece. In the four regions, the shape of the effective deformed region coincides with the shape of the target workpiece, and its size determines the efficiency of the forming process. The transition region acts as a buffer in the forming process so that the effective deformed region and rigid region can be gently connected and reduce the indentation of junction.

3 The design of the transition region

The design of the transition region is a key component in SMPF since it determines the quality of forming parts directly. The purpose of setting the transition region is to coordinate the forming of the sheet metal and shape of the workpiece, to make the deformation uniform, and to avoid local severe deformation in the transition and free deformed regions. Therefore, the design of the transition region needs to meet the following conditions. (1) The surface of the transition region is at least G2 continuous to ensure that it is smooth. (2) The positions of the effective deformed, transition, free deformed, and rigid regions need to be continuous. The connections of the transition region and the other three regions are at least G1 continuous and have a common tangent plane along each common connection line. (3) The design of the transition region should coordinate the effective forming area and rigid area. The change in the curvature cannot occur too fast in the transition region, and the height difference should be reasonable.

G0, G1, and G2 are the ways to describe the connection between surfaces or curves. The connection between the two

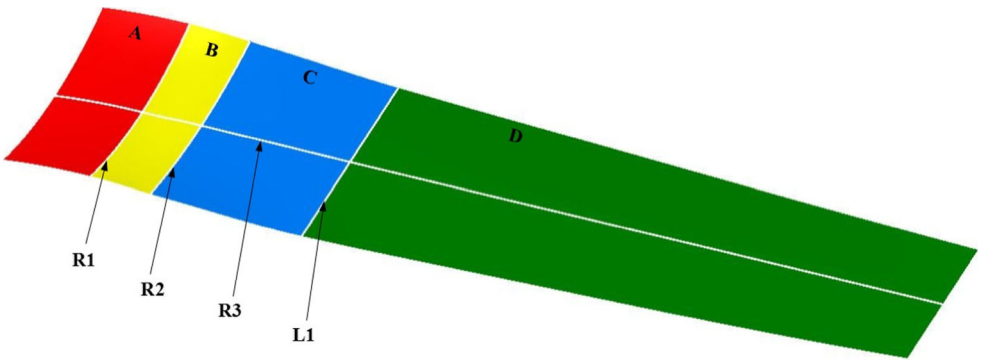

Fig. 2 Distribution of deformation regions in SMPF. (A) Effective deformed region, (B) transition region, (C) free deformed region, (D) rigid region. R1 boundary line of A and B regions, R2 boundary line of B and C regions, R3 middle ridge line

A- Effective deformed region; **B-** Transition region; **C-** Free deformed region; **D-** Rigid region
R1- Boundary line of A and B regions; **R2-** Boundary line of B and C regions; **R3-** Middle ridge line

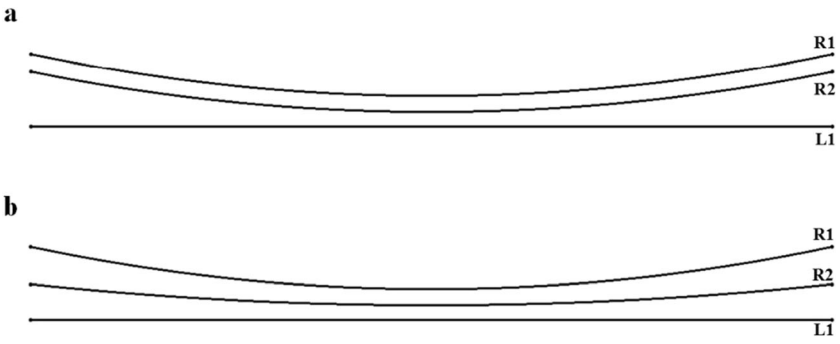

Fig. 4 The relationship of the curves in the width direction. **a** Without transition region design in the width direction. **b** With transition region design in the width direction

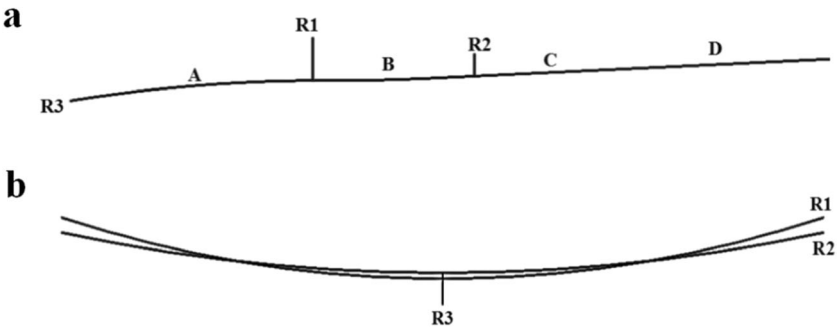

Fig. 5 With the design of transition region in the length direction. **a** Length direction. **(b)** Width direction

function curves $P(t)$ and $Q(t)$, as shown in Fig. 3, is illustrated as an example.

If it is required to reach the G0 continuity at the junction, the two curves are continuous in the location of the junction.

$$P(1) = Q(0)$$

If the G1 continuity is required at the junction, it means that the two curves meet the G0 continuity at the junction and have the common tangent.

$$Q'(0) = aP'(1)\ (a > 0)$$

If the G2 continuity is required at the junction, the two curves satisfy the G1 continuity at the junction and have the common curvature vector.

$$\frac{P'(1) \times P''(1)}{\left|P'(1)\right|^3} = \frac{Q'(0) \times Q''(0)}{\left|Q'(0)\right|^3}$$

In this paper, the forming of saddle-shaped parts is used as an example to illustrate the design of the transition region. The radius of curvature in the width and length directions of the parts is denoted r1 and r3, respectively. The radius of curvature of the curve labeled R2 is denoted r2 in Fig. 2. Then, the radius of curvature of the curve labeled R1 is r1, and the curvature of the curve labeled R1 is 1/r1 in Fig. 2. When the transition region is not designed, the radius of curvature of the curve labeled R2 is equal to that labeled R1 and the curvature of the curve labeled R2 is 1/r1 too (r1 = r2; 1/r1 = 1/r2). In the design of the transition region, it is necessary to optimize the curved surface in both the length and width directions. In the width direction, a buffer transition of curvature from 1/r1 to 0 from the effective deformed region to the rigid region is achieved by increasing the radius of curvature of the curve labeled R2. When the transition of curvature is the most reasonable, the plastic deformation of the sheet is the most stable in the transition and free deformed regions, and the forming result is best. To minimize the indentation between the transition

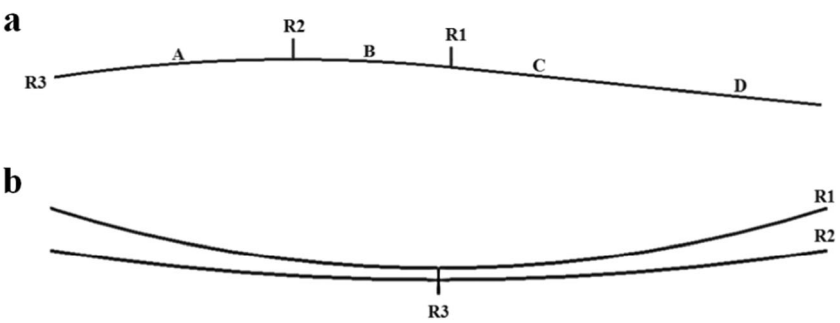

Fig. 6 Without the design of transition region in the length direction. **a** Length direction. **b** Width direction

Table 1 Mechanical parameters of 2024 aluminum alloy

Material	Density, ρ (kg/m^3)	Poisson ratio	Young's modulus, E (GPa)	Yield stress (MPa)
2024 aluminum alloy	2720	0.33	40.6	75.5

region and free deformed region, the difference in the length direction between the effective deformed region and free deformed region is reduced by designing a buffer transition connection in the transition region during SMPF. When the height difference is chosen to be the most reasonable, the plastic deformation of the sheet metal is the most stable in the transition and free deformed region, and the forming effect is best.

When there is not the design of the transition region in the length direction, Fig. 4 shows the curvature relationship among the curves in the width direction. The lack of design of the transition region in the width direction is illustrated in Fig. 4a, while presence of the design is in Fig. 4b. Referring to Fig. 2, in Fig. 4, the curve labeled R1 represents the junction boundary between the effective deformed region and transition region, and the curvature of the curve is 1/r1.The curve labeled R2 represents the junction boundary between the transition region and free deformed region, and the curvature of the curve is 1/r2. The line labeled L1 represents the line in the width direction of the rigid region, and the curvature of the curve is 0. Comparing Fig. 4a, b, when the transition region is designed in the width direction, the labeled curves in the width direction change from R1 to R2 to L1 and the curvature of the curves change from 1/r1 to 1/r2 to 0. To achieve the curvature of the curves evenly halved in the transition region, the radius of curvature of the curve labeled R2 is set to twice as much as that labeled R1 ($r2 = 2r1$; $1/r1 = 2/r2$). The changes in transition curvature are buffered, and deformation becomes more stable.

When there is the design of the transition region in the width direction, the curves R1, R2, and R3 (Fig. 2) are used to design the transition region in the length direction, as shown in Figs. 5 and 6. In Fig. 5a, the transition region is region B, and the effective deformed region A and free deformed region C are connected by transition region B. In the B region, one end of the middle ridge line is continuously connected with the line of region A through the G2 continuity, and the other end is continuously connected with the line of region C through the G1 continuity. The curve of region B maintains a continuous curvature. The curve labeled R1 is the junction boundary between the effective deformed region and transition region, while the curve labeled R2 is the junction boundary between the transition region and free deformed region. Figure 6 does not perform the design of the transition region in the length direction. Compared with Fig. 6b, adjusting the height difference between the curves R1 and R2 in Fig. 5b can coordinate the deformation of the middle and edge of the sheet metal to avoid the severe plastic deformation, reduce the indentation, and improve the forming effect.

4 Finite element analysis model

2024 aluminum alloy, a sheet material for shipbuilding, was used as the experimental material. The sheet metal and its performance parameters used in the experiment are provided by an aircraft manufacturer. The relevant material parameters are shown in Table 1.The density of the polyurethane pad is 1.26 g/cm^3, and the Marlow model is used to simulate in ABAQUS. The stress–strain curve is shown in Fig. 7a. In this model, it is assumed that the sheet metal is isotropic and uniform and obeys the von Mises yield criterion and the plastic flow rule. The stress–strain relation approximately obeys the exponential strengthening relation. The tensile test data of the plastic material was converted into a true stress–strain, and the curve is shown in Fig. 7b. The sheet metal used in this work

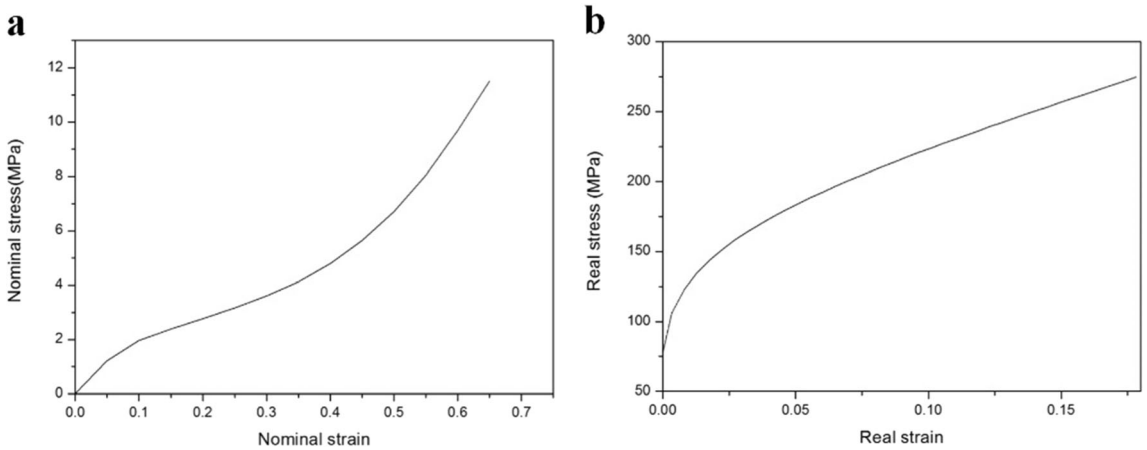

Fig. 7 Stress–strain curve. **(a)** Polyurethane pad. **(b)** 2024 aluminum alloy

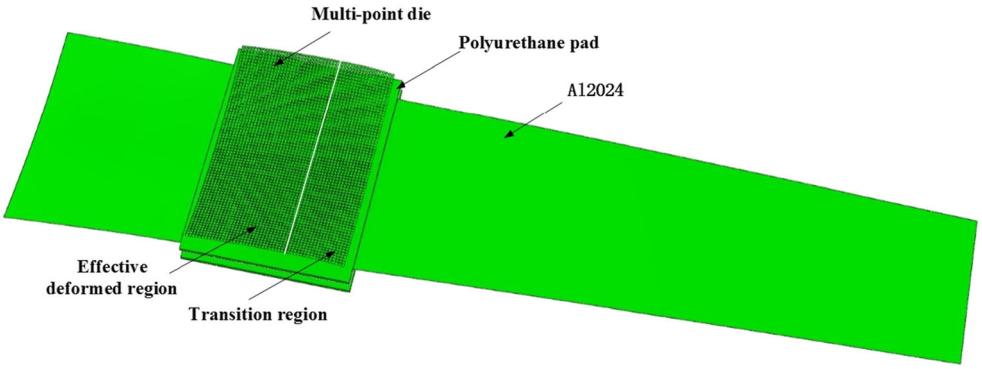

Fig. 8 The finite element model

was of isosceles trapezoid shape, where the upper bottom edge was 500 mm, lower bottom edge was 700 mm, and height was 3000 mm. The forming part was saddle-shaped, where the radii of curvature in the length and width directions were 2000 and 1200 mm, respectively.

In the finite element analysis models, punch and die elements adopted in the forming process were dispersed into R3D4 solid units, which are four-node bilinear tetrahedral discrete rigid elements. Polymer blankets were separated into C3D8R solid elements which are eight-node linear hexahedral, reduced integral elements, while the sheet metal was dispersed into reduced integral S4R shell elements. The algorithm of general contact was used in the sheet metal forming process, where the friction coefficient was considered to be 0.3. It was assumed that all the contact in the model obeyed the Coulomb friction model. The vertical direction of the punch was allowed a translational degree of freedom in the forming process, while rotation and translation in the other directions were restricted. Punch movement was controlled through the displacement-time curve. Figure 8 displays the finite element analysis model established by the finite element analysis software (ABAQUS), which consists of three groups: the multi-point die, polyurethane pad, and sheet metal. The basic body had a ball radius of 8 mm and length of 10 mm, the sheet metal thickness was 6 mm, and the size and thickness of the polyurethane pad were 740 × 540 and 10 mm, respectively.

5 Analysis of simulation results

Using the above finite element model, the finite element analysis software (ABAQUS) was used to simulate the sheet metal in two ways, including with and without the design of the transition region. Results of the two methods were analyzed and compared. The size of the effective deformed region in the experiment of simulation analysis determines the forming efficiency. The size of the transition region determines the

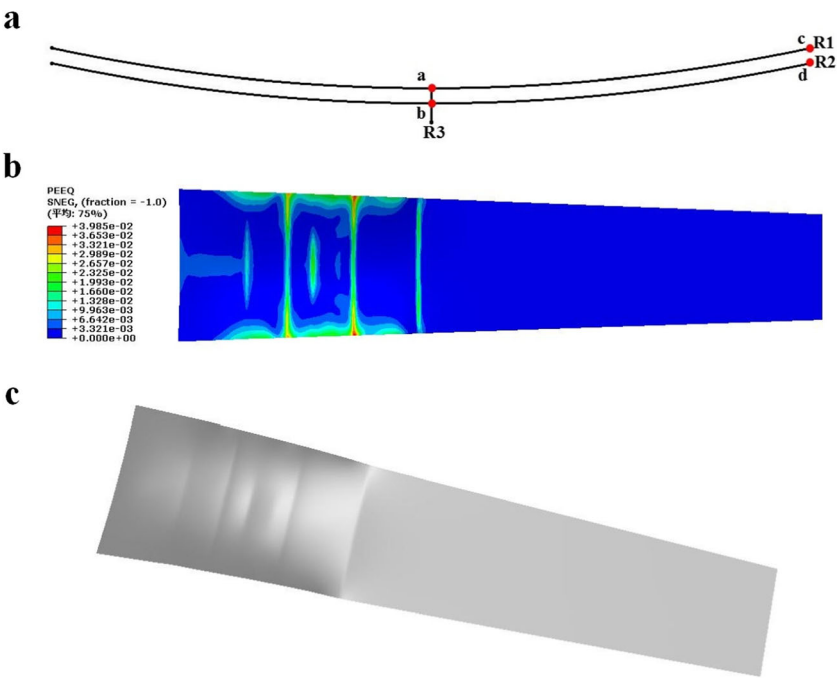

Fig. 9 Analysis without the design of transition region. **a** The curves in the width direction. **b** The strain distribution nephogram. **c** Illumination map of the part

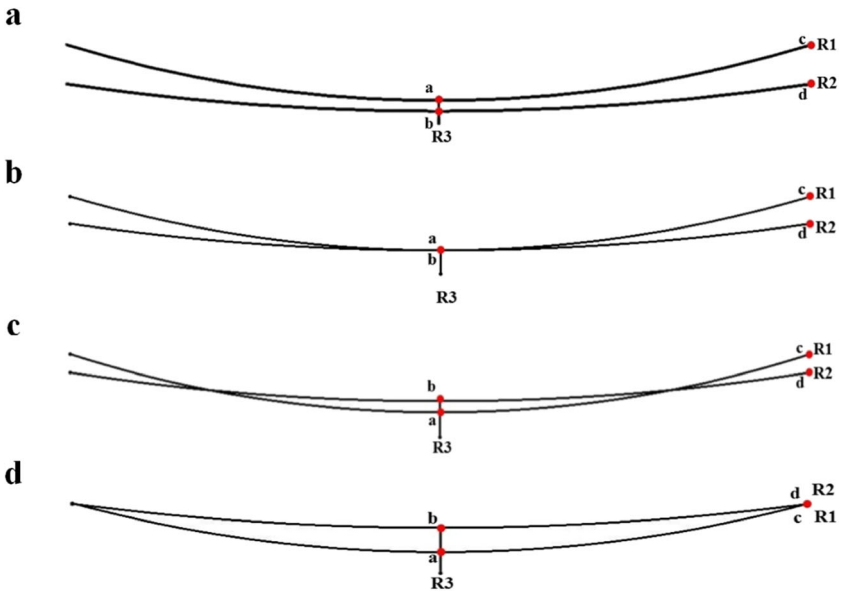

Fig. 10 The height difference of middle ridge line. **a** Height difference of middle ridge line was 10 mm (no height difference designed). **b** Height difference of middle ridge line was 0 mm. **c** Height difference of middle ridge line was − 13 mm. **d** Height difference of middle ridge line was − 26 mm

deformation and coordination in the forming process. In the simulation analysis experiment, the width of the effective forming and transition regions were 300 and 200 mm, respectively, which ensured the forming efficiency and facilitated coordinated deformation of the workpiece. According to the design and analysis of the transition region in the width direction, the radius of curvature of the curve labeled R2 was 2400 mm and was set to twice as much as that labeled R1 (r2 = 2r1; 1/r1 = 2/r2). The uniform transition of curvature from 1/r1 to 1/r2 to 0 was realized when the sheet metal was formed.

Figure 9a shows the method without the design of the transition region, where the radius of curvature of the curves labeled R1 and R2 were both 1200 mm. Curves R1 and R2 were parallel to each other in the width direction and had a height difference of about 10 mm, which is represented as H0 = a–b = c–d. Figure 9b presents the strain distribution nephogram without the design condition of the transition region and

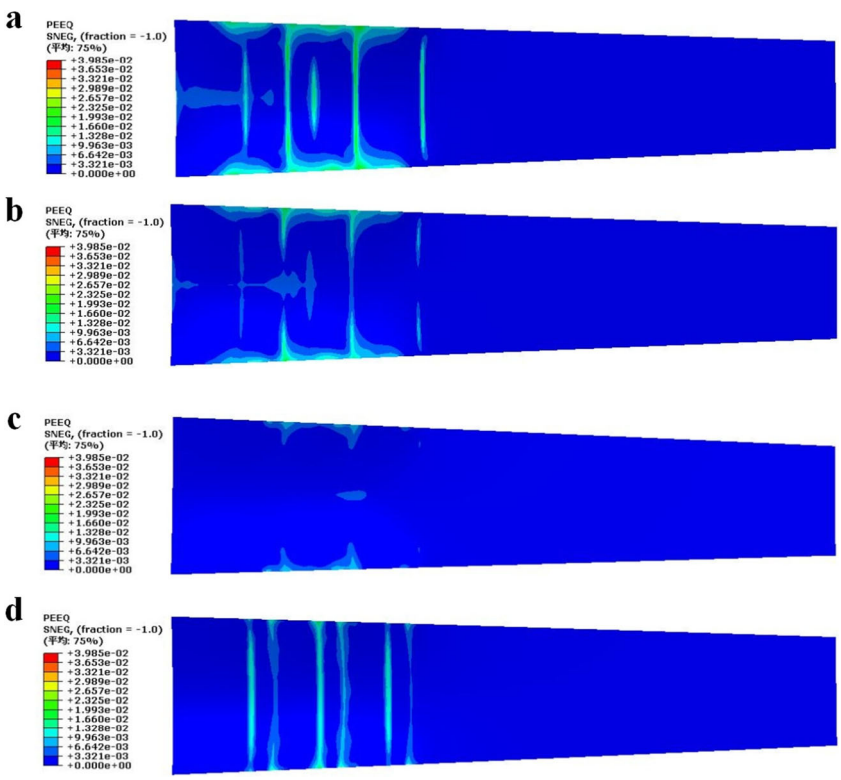

Fig. 11 The strain distribution nephogram. **a** Height difference of middle ridge line was 10 mm (no height difference designed). **b** Height difference of middle ridge line was 0 mm. **c** Height difference of middle ridge line was − 13 mm. **d** Height difference of middle ridge line was − 26 mm

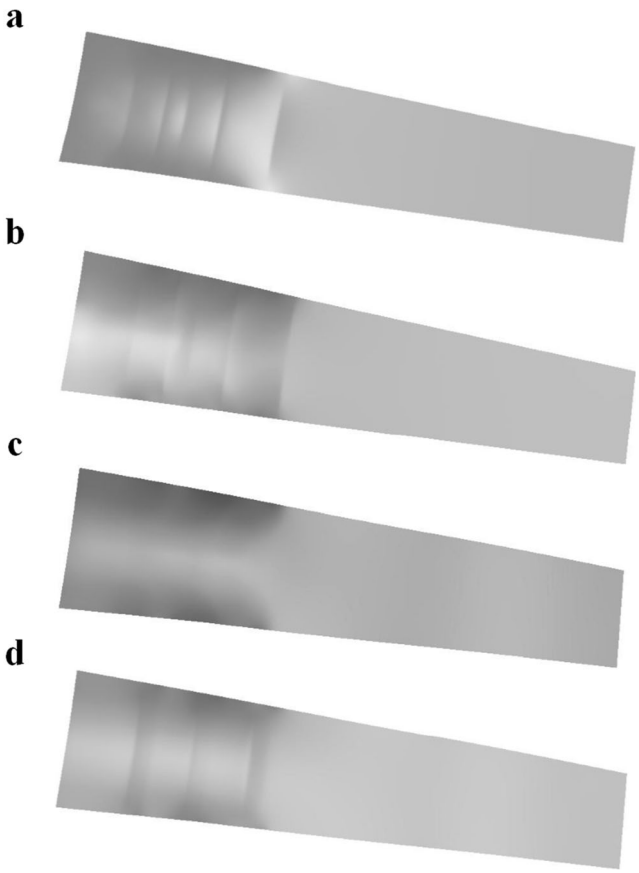

Fig. 12 Illumination maps of the parts. **a** Height difference of middle ridge line was 10 mm (no height difference designed). **b** Height difference of middle ridge line was 0 mm. **c** Height difference of middle ridge line was − 13 mm **(d)** Height difference of middle ridge line was − 26 mm

shows that strain was greatest at the junction boundary of the sheet metal. Figure 9c contains the Illumination map without the design condition of the transition region, which suggests that indentation was largest at the junction boundary of the sheet metal.

Figure 10 displays the methods with design of the transition region in the width direction, where the radius of curvature of the curve labeled R2 was 2400 mm. When the height difference was not designed in the transition region, the height difference between the curves labeled R1 and R2 was about 10 mm and represented as H1 = a–b in the middle ridge line of this model, which is the height difference between a and b in the graph. The height difference between the curves labeled R1 and R2, represented as H2 = c–d, in the edge line was about 36 mm, which is the height difference between c and d in the graph. When the height difference was designed in the transition region design, the height difference of the transition region was designed with the following three group parameters: H1 of 0 mm, H2 of 26 mm; H1 of −13 mm, H2 of 13 mm; and H1 of 26 mm, and H2 of 0 mm. Then, finite element analysis model was established for analysis and calculation in ABAQUS. The radius of curvature of the curve labeled R2 was 2400 mm, and the height differences in the middle ridge line between the curves labeled R1 and R2 were 10 mm (no transition region designed in the length direction) 0 mm, − 13 mm, and − 26 mm respectively in the model, which are the height differences between a and b in the graph. The simulation of the strain distribution nephogram was obtained by pressing three sections of sheet metal.

Figure 11 shows a comparison of the strain distribution nephogram under the design conditions of four different transition regions. From strain distribution nephogram, the strain at the junction boundary of the sheet metal was larger when the height difference was not designed (height difference of middle ridge line was 10 mm) and the height difference in the middle ridge line was − 26 mm. When the height difference between the curves labeled R1 and R2 in the middle ridge line was 0 mm, the strain obviously decreased at the junction boundary of the sheet metal. When the height difference between the curves labeled R1 and R2 in the middle ridge line was − 13 mm, the strain was the least at the junction boundary of the sheet metal.

Figure 12 presents a comparison of illumination maps under the design conditions of four different transition regions. The illumination maps suggest that when the height difference was not designed (Height difference of middle ridge line was 10 mm) and the height difference in the middle ridge line was − 26 mm, the indentation at the junction boundary of the sheet metal was larger. When the height difference between the curves labeled R1 and R2 in the middle ridge line was 0 mm, the indentation decreases at the junction boundary of the sheet metal. When the height difference between the curves labeled R1 and R2 in the middle ridge line was − 13 mm, the indentation at the junction boundary of the sheet metal was the least.

In summary, as shown in Fig. 13, when the curves of R1 and R2 crossed between the middle ridge line and the edge line in the width direction, the absolute value of the height difference in the middle ridge line was close to that in the edge line and the radius of curvature of the curve labeled R2 was set to twice as much as that in labeled R1; the plastic deformation of the sheet metal in the transition region was the most stable and the forming effect was best, further proving that design of the transition region was the most reasonable and necessary in this way.

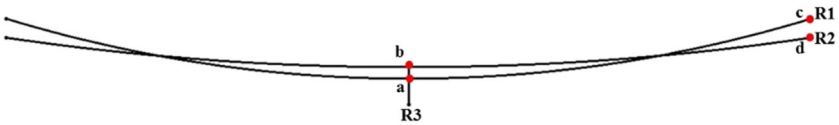

Fig. 13 The most reasonable relationships of the curves

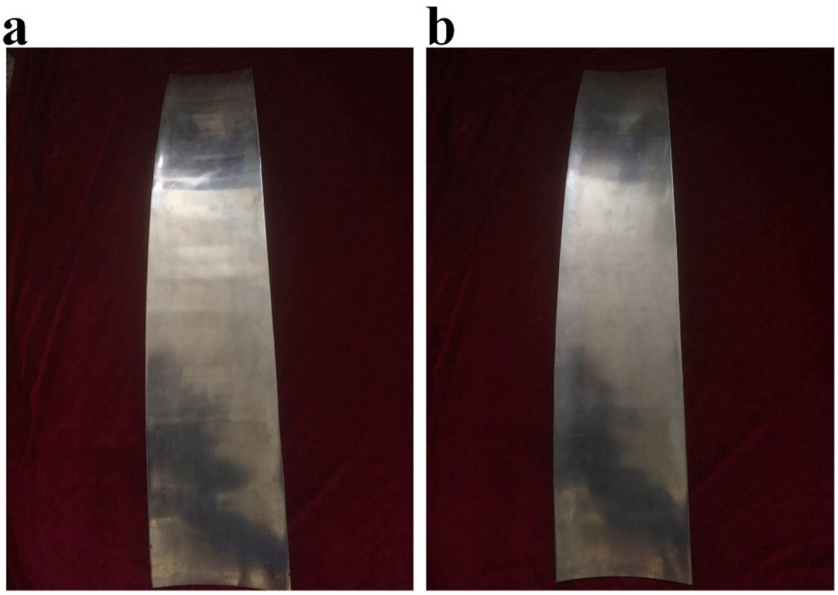

Fig. 14 2024 aluminum alloy forming parts. **a** Part without the design of transition region. **b** Part with the reasonable design of transition region

6 The experiments of SMPF

SMPF experiments were carried out on the YAM-200 multi-point forming press developed by Jilin University to verify the feasibility and versatility of the design of the transition region in the SMPF process. The pressure of the press was 40 T, and the saddle-shaped dies with and without design of the transition region were adjusted using shape adjustment equipment. Due to limitations of the experimental conditions, the actual experimental parameters were reduced threefold compared to the above simulation analysis experimental parameters. The parameters included the following: the size of the die was 240 × 170 mm, and the sheet metal was of isosceles trapezoid, where the size of the upper bottom edge was 167 mm, lower bottom edge was 233 mm, and height was 1000 mm. The radii of curvature in the length and width directions were 667 and 400 mm, respectively. The length of the transition region was 67 mm, and the thickness of the 2024 aluminum alloy steel sheet was 2 mm.

Figure 14a shows a picture of experimental part without design of transition region, while Fig. 14b contains a picture of experimental part with the most reasonable design of the transition region. Without design, there were obvious indentations at the junction boundary at each section of the sheet metal. With the reasonable design of the transition region, the surface of the forming part was smooth, indentations were obviously reduced, and the forming quality was good.

7 Conclusion

(1) SMPF technology combines the sectional forming technology with MPF technology. Applying sectional forming reduces the indentation at the junction boundary of the sheet metal during the sectional forming by setting a reasonable transition region. The forming quality of the sheet metal can be improved, and the forming process of large-size sheet metal can be realized.

(2) With the design of the transition region, height difference between the transition region and the radius of curvature of the transition region affects the design of the transition. Good transition height difference and transition radius of curvature are favorable to obtain a smooth transition between the effective deformed region and the rigid region of the sheet to avoid local severe plastic deformation.

(3) This presented experimental study on 2024 aluminum alloy sheet metal compares methods with and without design of the transition region and proves that SMPF of sheet metal is most valid and feasible with the design.

References

1. Cai ZY, Li MZ (2002a) Multi-point forming of three- dimensional sheet metal and the control of the forming process. Int J Press Vessel Pip 79(4):289–296
2. Abosaf M, Essa K, Alghawail A, Tolipov A, Shizhong S, Pham D (2017) Optimisation of multi-point forming process parameters. Int J Adv Manuf Technol 92:1849–1859
3. Abebe M, Lee K, Kang B-S (2016) Surrogate-based multi-point forming process optimization for dimpling and wrinkling reduction. Int J Adv Manuf Technol 85:391–403
4. Cai ZY, Li MZ, Chen XD (2006) Digitized die forming system for sheet metal and springback minimizing technique. Int J Adv Manuf Technol 28:1089–1096
5. Jia BB, Wang WW (2017) New process of multi-point forming with individually controlled force-displacement and mechanism of inhibiting springback. Int J Adv Manuf Technol 90:3801–3810
6. Li MZ, Liu CG, Chen QM (2000) Multi-point forming for large size 3D sheet metal parts. Electromachining Mould 2:42–44

7. Bai Y, Zhang YY, Zhao G, Chen L (2011) Research on precise forming process of aircraft aluminum large sheet metal part. Forging Stamping Technol 36(4):64–67
8. Moshaiov A, Vorus WS (1987) The mechanics of the flame bending process: theory and applications. J Ship Res 31(4):266–275
9. Dong DS, Liu CG, Tan JH (2002) The research of line heating deformation. Mar Technol 156(1):29–33
10. Sui Z, Liu CG, Cui XJ, Li MZ, Liu W (2003) Development of feed-in device for multi-point forming of sheet metal. J Jilin Univ Technol 33(1):17–21
11. Ma RY, Ding H, Yang DY (2014) Research and design of an equipment for multi-point press forming sheet metal parts. Key Eng Mater 575-576:467–471
12. Sui Z, Liu CG (2003) Development of control system for rapid shape adjusting multi-point forming press. J Plast Eng 10(5):53–58
13. Fu WZ, Li MZ (2003) Study on 100 KN multi-point forming press and sectional forming process. Trans Chin Soc Agric Mach 34(5): 186–188
14. Chen JJ, Li MZ (2000) Multi-point section forming technology. J Harbin Inst Technol 32(4):65–71
15. Peng HL, Li MZ, Liu CG, Cao JH (2013) Study of multi-point forming for polycarbonate sheet. Int J Adv Manuf Technol 67: 2811–2817
16. Liu YJ, Li MZ, Ju FF (2017) Research on the process of flexible blank holder in multi-point forming for spherical surface parts. Int J Adv Manuf Technol 89:2315–2322

Publisher's Note